Separation Science and Technology
Publication details, including instructions for authors and subscription information:
http://www.informaworld.com/smpp/title~content=t713708471

Outlet Stream Splitting for Sample Concentration in Field-Flow Fractionation

J. Calvin Giddings[a]; Hao-Chao Lin[a]; Karin D. Caldwell[a]; Marcus N. Myers[a]
[a] DEPARTMENT OF CHEMISTRY, UNIVERSITY OF UTAH, SALT LAKE CITY, UTAH

To cite this Article Giddings, J. Calvin , Lin, Hao-Chao , Caldwell, Karin D. and Myers, Marcus N.(1983) 'Outlet Stream Splitting for Sample Concentration in Field-Flow Fractionation', Separation Science and Technology, 18: 3, 293 — 306
To link to this Article: DOI: 10.1080/01496398308058338
URL: http://dx.doi.org/10.1080/01496398308058338

SEPARATION SCIENCE AND TECHNOLOGY, 18(3), pp. 293–306, 1983

Outlet Stream Splitting for Sample Concentration in Field-Flow Fractionation

J. CALVIN GIDDINGS, HAO-CHAO LIN, KARIN D. CALDWELL, and MARCUS N. MYERS

DEPARTMENT OF CHEMISTRY
UNIVERSITY OF UTAH
SALT LAKE CITY, UTAH 84112

Abstract

Retention in field-flow fractionation is a result of a field-induced sample concentration in the vicinity of a channel wall. By splitting the channel flow at the exit, so that sample containing flow lines leave the channel at a different port than those free of sample, one may markedly enhance the detectability of a given sample. The enhancement is discussed for the cases of "ideal splitting," where an obstacle inserted in the flow stream affects the split, and "nonideal splitting," where the flow is caused to split at some level in the channel specified by the relative resistance to flow through the two outlets. The proposed increase in detector response through stream splitting is experimentally verified.

INTRODUCTION

Field-flow fractionation (FFF) is an analytical separation technique which is particularly promising for the isolation and characterization of small quantities of macromolecules and small particles (*1–3*). However, like chromatography, the applicability of FFF to certain trace-level components is limited by the availability of a detector sensitive enough to work with minute quantities. The detector problem is perhaps even more severe with FFF because it is more easily overloaded than chromatography, suggesting smaller initial samples. This is a consequence of the basic mechanism of FFF in which the solute material is all concentrated in one region of a carrier flow stream, usually near the wall of a flow channel. The solute components

0149-6395/83/1803-0293$3.50/0

then migrate downstream in the immediate vicinity of the wall, still highly concentrated. Prior to detection, the carrier and the concentrated solute are routed into connecting tubing where they are remixed over the flow cross-section and, in this diluted form, passed through a detector. The concentration process within the channel tends to increase solute–solute interactions and thus nonlinear or overloading effects, and the remixing step tends to dilute the solute and make detection more difficult.

The object of this paper is to show that the basic concentration mechanism of FFF, which amplifies the overloading problem, leads rather directly to a technique for reducing the very overloading effect it creates by improving sample detectability. Basically, this technique involves dividing the carrier flow stream at the outlet of the FFF channel in such a way that the concentrated solute near one wall is split away from the rest of the carrier stream (see Fig. 1). The concentrated solute stream is then fed to a detector and/or collector where it provides a greatly enhanced signal and/or a more concentrated sample cut. Because the detector signal is greatly enhanced,

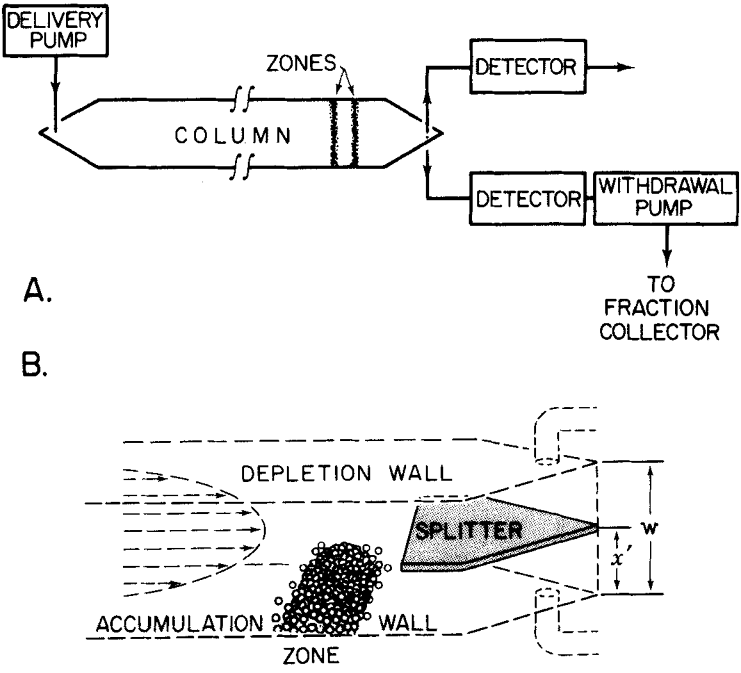

FIG. 1. Schematic diagram of (A) FFF column and ancillary equipment and (B) configuration of splitter in FFF flow channel.

sample quantities can be correspondingly reduced in order to decrease overloading. Alternatively, the enhanced signal can be used to more successfully study trace-level components in an initial sample of a fixed size.

THEORY

The principle of field-flow fractionation has been described in detail elsewhere (*1–3*). Generally, the FFF flow channel is a thin ribbonlike duct of rectangular cross-section with an aspect ratio (breadth/thickness) of 40 or more. A field is applied in a direction perpendicular to the channel, forcing the entrained solute to migrate toward one channel wall. The migration is halted by the wall, where the migrants are forced to accumulate. This accumulation is offset by diffusion and as a result steady-state solute layers are formed with a finite mean thickness l which is uniquely determined by the ratio of the diffusivity D to the field induced velocity U for each solute constituent: $l = D/U$. Expressed in terms of l, the concentration profile $c(x)$ has the following form:

$$c(x) = c_0 \exp(-x/l) \tag{1}$$

in which c_0 is the concentration at the accumulation wall where distance coordinate x equals zero.

The channel flow, which moves in a direction perpendicular to the field, carries the various solute layers downstream differentially at individual velocities which decrease with decreasing l values. This differential movement is the source of the separation process.

The retention of a zone of a given component is described by the dimensionless retention ratio R defined as

$$R = v_{\text{zone}}/\langle v \rangle \tag{2}$$

where v_{zone} is the downstream velocity of the zone and $\langle v \rangle$ is the average velocity of the (nonretained) carrier. The relationship between R and the zonal layer thickness l can be described exactly; it is most conveniently expressed in terms of the dimensionless parameter λ, which equals the ratio of l to channel thickness w:

$$R = 6\lambda[\coth(1/2\lambda) - 2\lambda] \tag{3}$$

Equation (3) has been extensively verified under a wide variety of fields (*3*–*5*).

When the sample is particulate with particle dimensions which exceed the layer thickness l, the retention becomes governed by the particle radius rather than by l. In this case larger particles slide or roll downstream at a faster rate than smaller ones, opposite to the normal trend. Under this type of fractionation behavior, which we call steric FFF (*7*, *8*), all particles constituting a given component zone are again found in the immediate vicinity of the wall. In this case the retention ratio is given by

$$R = 6\gamma a/w \tag{4}$$

where a is the particle radius and γ is a velocity-dependent factor whose value is ideally close to unity.

The nonuniform cross-sectional distribution of solute, which is the basis for FFF retention, can be utilized to enhance detectability of the zones. By splitting the channel flow at some distance x_s from the accumulation wall, it is possible to elute the separated zones in concentrated form, i.e., without remixing with the bulk of nearly pure carrier located near the depletion wall (Fig. 1B).

We will discuss first the case of *ideal splitting*, in which the volumetric flow rates through the two branches of the flow stream are adjusted so that the undivided flow stream is not required to swerve out of its parallel path (except to divide around the finite width of the splitter) in order to discharge into one or another of the two branches. Both ideal and nonideal situations are illustrated in Fig. 2. In this figure, flows are shown as they divide around the splitter, with $\dot{V}$ the total volumetric flow rate and $\dot{V}_s$ being that part which is split off with enriched sample.

In the case of ideal splitting, the positioning of the split will have direct bearing on the enhancement of the detector response to a given zone, since a split closer to the accumulation wall will result in the collection of more concentrated solute. This condition is covered by the following quantitative development.

For normal FFF, the fraction f of a given component which is located below a certain reduced split coordinate x_s/w, and thus collected in ideal splitting, is expressed as the ratio of the following integrals of concentration $c(x)$:

$$f = \int_0^{x_s} c(x)\ dx \Big/ \int_0^{w} c(x)\ dx \tag{5}$$

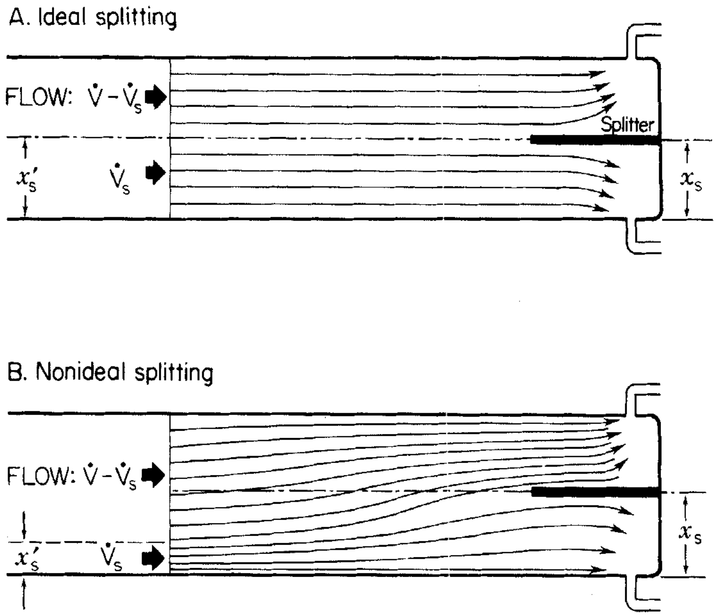

FIG. 2. Illustration of ideal and nonideal splitting. Volumetric flow rates above and below distance x_s' are indicated by $\dot{V} - \dot{V}_s$ and $\dot{V}_s$, respectively.

Integration yields

$$f = (1 - e^{-x_s/\lambda w})/(1 - e^{-1/\lambda}) \tag{6}$$

The degree of enrichment E of solute, which should also represent the enhancement factor for detector signal, is

$$E = \frac{f}{\dot{V}_s/\dot{V}} = \frac{\dot{V}(1 - e^{-x_s/\lambda w})}{\dot{V}_s(1 - e^{-1/\lambda})} \tag{7}$$

where $\dot{V}_s/\dot{V}$ is the fraction of the total volumetric flow $\dot{V}$ emerging as the enriched stream.

In the limit of no retention, for which $\lambda \rightarrow \infty$, E approaches unity, as expected. For reasonably retained peaks, $\lambda \ll 1$ and $e^{-1/\lambda}$ is negligible, giving

$$E = (\dot{V}/\dot{V}_s)(1 - e^{-x_s/\lambda w}) \tag{8}$$

For most such retained peaks, it will be impractical to make the volumetric split ratio $\dot{V}_s/\dot{V}$ small enough (for reasons to be explained later) to approach the smallness of λ, in which case $e^{-x_s/\lambda w}$ will also be negligible. In this case we have the simple limiting form

$$E = \dot{V}/\dot{V}_s \tag{9}$$

The latter equation will also generally apply to steric FFF, but care must be taken that x_s is substantially larger than the particle diameter to avoid clogging, and that the lift forces of steric FFF are not sufficient to carry the particles over the stream splitter.

Clearly, both f and E are influenced by parameter λ to some degree, and thus, through Eq. (3), by retention ratio R. Figure 3 shows variations in f with reduced split coordinate x_s/w for a series of different R's. A split in the middle of the channel ($x_s/w = 0.5$) is seen to funnel a full 99% of even a weakly retained solute ($R = 0.5$) through the exit port of the accumulation wall. A split at x_s/w of 0.25 for the same solute retained to the same degree results in a loss of 9% of the solute.

Figure 4 shows the degree to which the enrichment (enhancement) factor E departs from its limiting form $\dot{V}/\dot{V}_s$ (Eq. 9) as a function of the reduced split coordinate x_s/w. The figure shows that the departures from $\dot{V}/\dot{V}_s$ are not substantial except for very (usually impractically) small x_s/w values, or for very weak retention with R approaching unity.

We note now that the above equations and plots can be adapted to the case of *nonideal splitting.* For this purpose we note that upstream of the splitter, where the flow is not yet perturbed by the splitter, there is some coordinate distance x_s' which serves as the true split point between fluid divided into the two streams. For ideal splitting, $x_s' = x_s$, whereas for nonideal splitting, $x_s' \neq x_s$. These two cases are illustrated in Fig. 2. In order to describe nonideal splitting, we must simply replace x_s in all the foregoing equations and plots by x_s'. In order to relate the split coordinate x_s' of ideal or nonideal splitting to the diverted flow rate $\dot{V}_s$, we must establish the general relationship of flow to the lateral coordinate x.

The volumetric flow rate $\dot{V}_s$ of the enriched stream consists of that of the entire flow below coordinate x_s', which is

$$\dot{V}_s = b \int_0^{x_s'} v \; dx \tag{10}$$

where b is the breadth of the channel and v is the local stream velocity, the latter related to coordinate x as follows for normal parabolic flow (*9*):

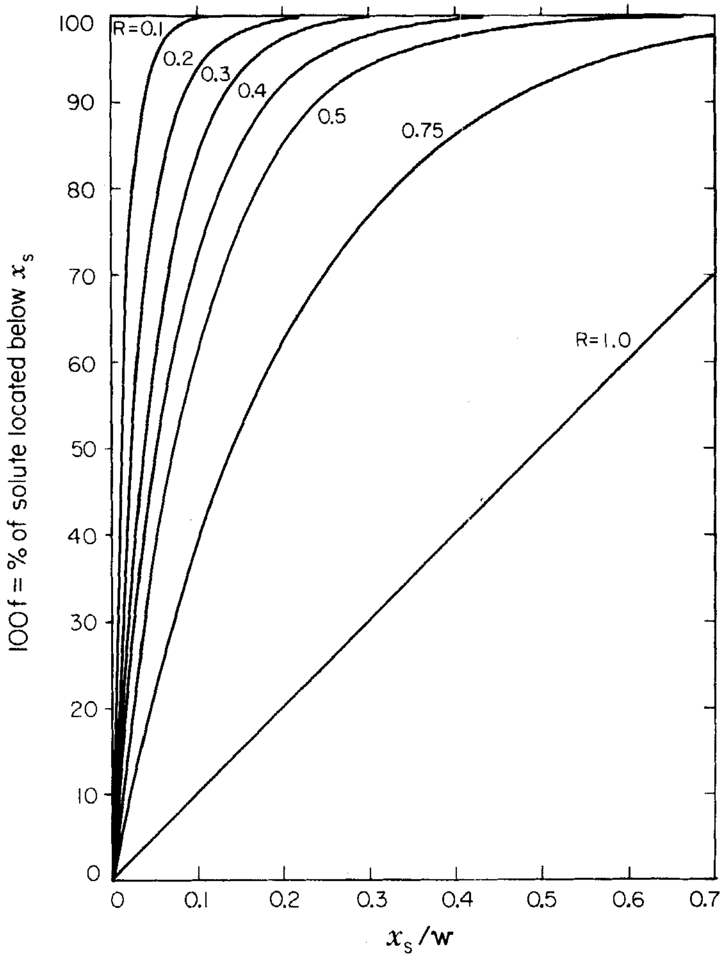

FIG. 3. Plot showing percentage of a given solute (associated with a specific R value) located below coordinate position x_s in the FFF channel.

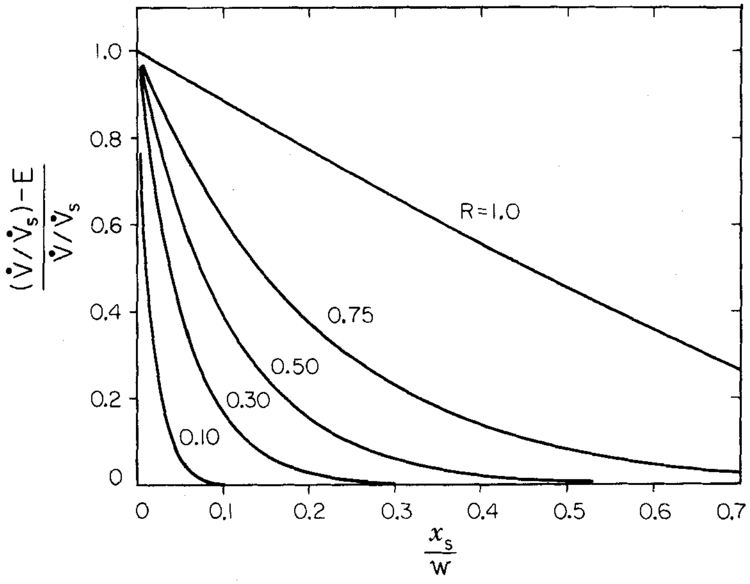

FIG. 4. Plot of departure of enrichment factor E from limiting value $\dot{V}/\dot{V}_s$ as a function of x_s/w.

$$v = 6\langle v \rangle \left[\frac{x}{w} - \left(\frac{x}{w}\right)^2\right] \tag{11}$$

The substitution of Eq. (11) into (10), followed by integration, yields

$$\dot{V}_s = 3bw\langle v \rangle \left[\left(\frac{x_s'}{w}\right)^2 - \frac{2}{3}\left(\frac{x_s'}{w}\right)^3\right] \tag{12}$$

The total volumetric flow rate of the channel is given by the above expression with x_s' replaced by w:

$$\dot{V} = bw\langle v \rangle \tag{13}$$

The last two equations provide the fraction of flow diverted into the enriched stream:

$$\frac{\dot{V}_s}{\dot{V}} = 3\left[\left(\frac{x_s'}{w}\right)^2 - \frac{2}{3}\left(\frac{x_s'}{w}\right)^3\right] \tag{14}$$

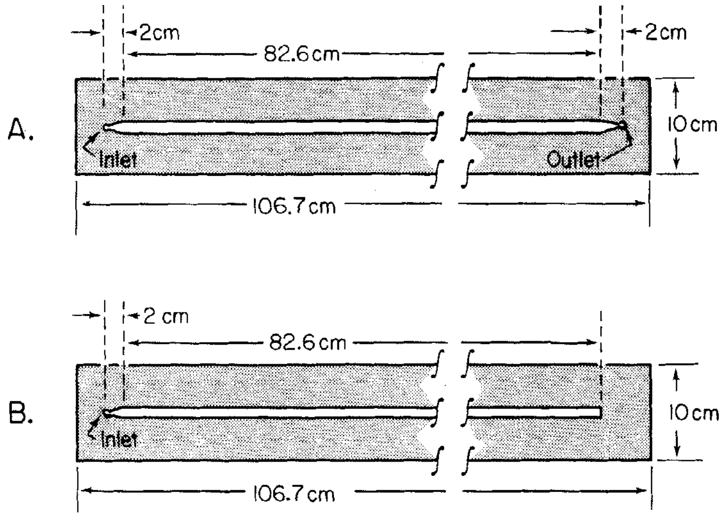

FIG. 5. Configuration of Mylar spacers used to construct the FFF channel with split outlet. Spacer B, 51 μm thick, is sandwiched between two sheets of A, each 127 μm thick. The blunt end of B forms the stream divider within the sandwich construction.

This equation can be used to relate the effective split coordinate x_s' to the magnitude of the flow $\dot{V}$ diverted to the enriched exit port.

EXPERIMENTAL

The column we use to test the stream splitting concept is designed for steric field-flow fractionation. Thus it is designed for use with particles larger than 1 μm whose density is sufficiently different from that of the carrier to allow rapid settling to the lower channel wall under the influence of gravity. While steric FFF provides the simplest test of stream splitting, the concept is also applicable to normal FFF, as noted in the theory section.

The general set-up of the FFF system is shown in Fig. 1A. The column consists of two 42" (106.7 cm) × 4" (10.2 cm) × 1/2" (1.27 cm) glass plates clamped over an arrangement of Mylar sheets cut to form the outline of the channel (see Fig. 5). Two 0.005" (127 μm) thick sheets outline the standard configuration of an FFF channel (Fig. 5A) with its tapered inlet and outlet.

The third sheet, 0.002" (51 μm) thickness, which has one blunt rather than tapered end (see Fig. 5B), is positioned between the other two in the assembled column. It is this blunt end which serves as a stream splitter when liquid is flowing through the column. The whole column, i.e., the three Mylar sheets surrounded by the glass plates, is held together by two clamping blocks of Plexiglas, as described previously (*6*). The channel void volume V^0 was calculated as 2.58 mL. Actual determinations through injections of acetone gave a value for V^0 of 2.53 mL, in good agreement with the above value.

Through the upper glass plate of the column, holes are drilled to accommodate the Teflon tubing (0.3 mm i.d.) by which carrier fluid enters and exits the column. These tubes are positioned at the apex of the tapered regions in the spacer. Through the bottom plate a similar Teflon tube is mounted for the exit of enriched solute.

Carrier liquid was fed to the channel by means of a Cheminert metering pump from Laboratory Data Control. The effluent from the pump was passed through a pulse dampener of coiled Teflon tubing before entering the column. Both the top and bottom outlets were connected to UV detectors from Laboratory Data Control, which monitored the absorbance/scattering of the effluent at 254 mm. The effluent through the bottom wall was regulated by a peristaltic pump from Gilson positioned after the detector; a pulse dampener of coiled Teflon tubing was placed between the detector and pump. A solution of 0.1% (v/v) FL-70 detergent from Fisher Scientific Inc. in distilled water was used as carrier throughout the experiment. The sample consisted of rather monodisperse silica spheres with dimensions of 5.6 ± 0.9 and 7.5 ± 0.9 μm, respectively. These beads were a gift from Dr J. J. Kirkland of E. I. du Pont de Nemours & Co. (Wilmington, Delaware). The particles were suspended in the carrier to concentrations between 2.5–3.5% (w/v). Injection volumes were kept at 2 μL of stirred suspension throughout the study. Injections were made at a channel flow of 2.8 mL/h; 0.2 mL of effluent was collected before the channel flow was stopped to allow settling of the particles. After 15 min of stopped flow, the pumps were again started at the flow rates selected for the particular run.

RESULTS AND DISCUSSIONS

A mixture of the two silica samples (diameters 5.6 and 7.5 μm) was first separated by the steric FFF system operated without splitting, i.e., with all effluent exiting through the bottom port. The samples were well resolved, as seen in Fig. 6A, but the amplitude of the peaks was low with a rather unfavorable signal-to-noise ratio. The retention ratio R for both components could, however, be determined, and amounted to 0.045 and 0.035 for the 7.5 μm and the 5.6 μm beads, respectively.

The top exit was subsequently opened to split the effluent, and the

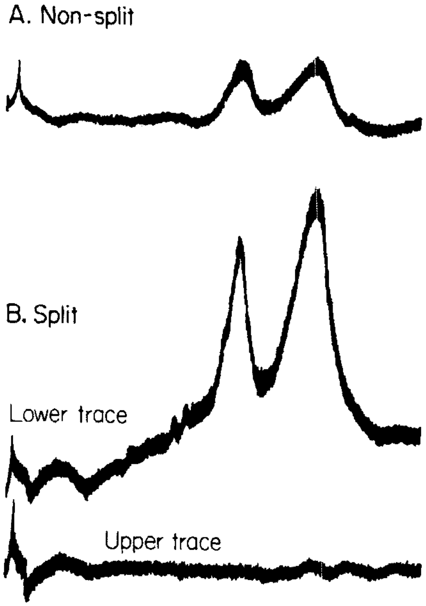

FIG. 6. Fractograms from nonsplit and split channel flows using the same sample size (2 μL) and overall flow rate ($\dot{V} = 60.7$ mL/h). In B, only 25% of the flow is diverted through the lower enriched channel, giving a fourfold signal enhancement compared to A. The detector trace for the upper channel, devoid of solute, shows no discernable peaks.

peristaltic pump at the bottom exit was set to withdraw one-quarter of the total column flow $\dot{V}$, which was maintained at the same level as before the split.

The fractograms recorded at the top and bottom ports are shown in Fig. 6B. The recorder trace corresponding to the lower exit port is seen to display a fourfold increase in peak amplitude predicted by Eq. (9), whereas the trace from the top exit shows no evidence of particles. The degree of retention of each of the two components appears unaffected by the split.

Since the sample is relatively dilute, one may safely assume Beer's law to be valid so that the detector signal at any point in the elution peak is proportional to the sample concentration at that point. For the purpose of comparison between runs, the peak maximum is usually the point of least ambiguity and is thus suitable as a point of reference for the measurement of detector response. According to Eq. (9), the detector response (proportional to E) at the maximum, or at any other corresponding point, should be proportional to $\dot{V}/\dot{V}_s$. Figure 7 shows a plot of the detector response (expressed as E) as a function of $\dot{V}/\dot{V}_s$ for the 7.5-μm silica beads. These

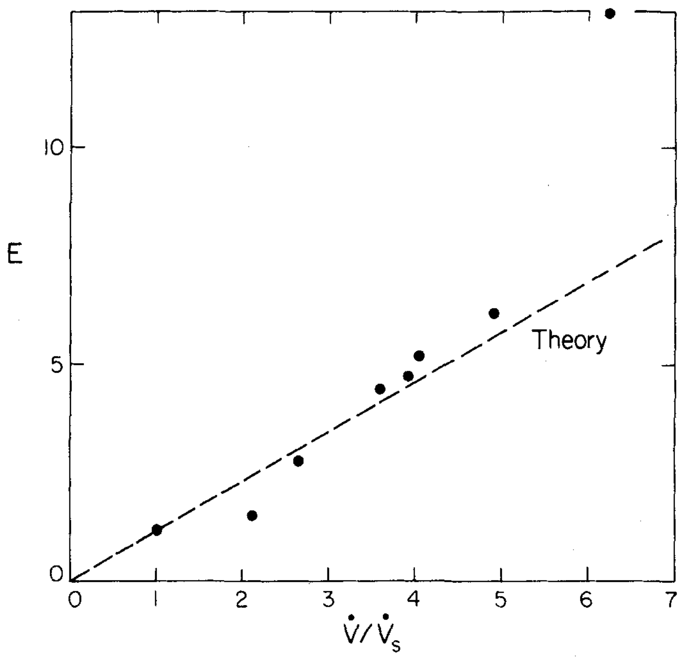

FIG. 7. Enrichment E, as measured by the enhancement of the detector signal for 7.5 μm silica beads at the peak maximum, as a function of $\dot{V}/\dot{V}_s$. The theoretical line is from Eq. (9), $\dot{V} = 71$. mL/h.

experiments were done by maintaining $\dot{V}$ at 71 mL/h and by varying $\dot{V}_s$. Although the experimental data do not show a perfect linear relationship, the trend of changes in detector response with $\dot{V}/\dot{V}_s$ is roughly as expected.

This set of experiments shows that stream splitting may be a useful technique for enhancing solute detectability in FFF systems, and for producing concentrated sample fractions in case further analysis is required. Although the technique is demonstrated here for a steric FFF system, it should prove generally useful for other FFF methods.

Along with the rather straightforward applications of outlet stream splitting, some rather interesting variations suggest themselves. For example, where some components of a sample are only poorly retained and thus relatively evenly distributed across the thickness of the channel, and others are heavily compressed against the channel wall, it may prove useful to vary the degree of flow splitting during a run. For the first few column volumes of effluent (e.g., until $R = 0.5$), one might refrain from splitting by collecting all effluent through one exit port. According to Fig. 3, one can at this point split the flow in half and thereby collect more than 98% of the sample through the accumulation wall exit. The pump which regulates the flow at this exit could then be programmed to gradually reduce V_s in order to maximize sample detectability. This scheme would be particularly useful if the later peaks were low in amplitude, thus needing detector enhancement, but broad enough so that the resolution loss accompanying extreme splitting was of no great importance.

Another variation of outlet stream splitting stems from the realization that some components may migrate along one wall and others along the other wall depending on differences in density, etc. Thus where there is a considerable overlap in the distribution of the two populations, an outlet stream splitter will serve to keep the two populations separate and to provide a separate distribution for each of them (*10*).

We now note that there is an important limitation to outlet stream splitting, particularly when carried to the extreme. Stream splitting, in reducing the volume of effluent in which component zones are collected, makes the zones more subject to distortion and broadening due to dead volume effects in the detector and connecting tubing. The distortion is the same as if the column void volume were reduced from V^0 to an effective volume of $V^0(\dot{V}_s/\dot{V})$. Thus all the care that must be applied to avoid the extraneous broadening of peak from low volume columns must also be applied to split outlet columns of the same "effective" volume.

Finally, we note that the application of our equations for f and E to nonideal splitting rests on the assumption that the solute above coordinate position x_s' (see Fig. 2B) will flow above the splitter and vice versa. However, solute relaxation may in some case be so fast as to distort this distribution in the short distance over which the streamlines swerve to divide around the splitter.

Acknowledgment

This material is based upon work supported by the National Science Foundation under Grant CHE 79-19879.

REFERENCES

1. J. C. Giddings, M. N. Myers, F. J. F. Yang, and L. K. Smith, *Colloid and Interface Science,* Vol. IV (M. Kerker, ed.), Academic, New York, 1976.

2. J. C. Giddings, S. R. Fisher, and M. N. Myers, *Am. Lab.,* p. 15 (May 1978).

3. J. C. Giddings, *Anal. Chem., 53,* 1170 (1981).

4. G. Karaiskakis, M. N. Myers, K. D. Caldwell, and J. C. Giddings, *Ibid., 53,* 1314 (1981).
5. J. C. Giddings, K. D. Caldwell, and M. N. Myers, *Macromolecules, 9,* 106 (1976).
6. J. C. Giddings, M. N. Myers, K. D. Caldwell, and S. R. Fisher, in *Methods of Biochemical Analysis*, Vol. 26 (D. Glick, ed.), Wiley, New York, 1980, p. 79.
7. J. C. Giddings and M. N. Myers, *Sep. Sci. Technol., 13,* 637 (1978).
8. M. N. Myers and J. C. Giddings, *Anal. Chem., 54,* 2284 (1982).
9. J. Happel and H. Brenner, *Low Reynolds Number Hydrodynamics,* Prentice-Hall, Englewood Cliffs, New Jersey, 1965, p. 34.
10. F. S. Yang, PhD Thesis, University of Utah, 1981, p. 102.

Received by editor August 27, 1982